DETECTING PATTERNS OF STRUCTURE FORMATION AT VARIOUS TYPES OF METAL MACHINING

Проведено дослідження впливу різних видів термічного різання, а саме аргоно-плазмового, повітряно-плазмового та киснево-флюсового різання, на закономірності формування зони термічного впливу та структуроутворення в зоні різу. Детально проаналізовано формування структурних складових термооброблених шарів по глибині зони термічного впливу після різних видів термічного різання для сталей різного ступеню легування. Встановлено, що у результаті термічного різання утворюються умовні ділянки, які характеризуються різними структурними складовими залежно від хімічного складу сталей та типу обробки. В дослідженні представлено особливості фазових та структурних перетворень при термічному різанні сталей. Показано вплив способу термічного різання на формування структурних складових як у зоні оплавлення, так і на ділянках, що знаходяться поблизу основного металу. Приведено вплив способу різання на глибину оплавленої та перехідної ділянок. Описано явища, пов'язані з процесом кристалізації після різання. Детально розглянуто вплив швидкості охолодження на структуру металів в зоні різання для широкого спектру марок сталі. Встановлено основні закономірності структуроутворення при кристалізації оплавленого металу в зоні різу залежно від обраного способу термічного різання. Показано вплив способу термічного різання на зміну мікротвердості поверхні різу та на глибину термічно оброблених шарів. Показано, що вибір у якості технологічної операції методу повітряно-плазмового різання дозволяє значно знизити глибину зони термічного впливу та мікротвердість у зоні різу порівняно з аргоно-плазмовим та киснево-флюсовим різанням. Доведено ефективність технологічного процесу повітряно-плазмового різання у порівнянні з іншими розглянутими методами за рахунок зменшення глибини зони термічного впливу, що обумовлює зниження трудових та економічних витрат на подальшу обробку поверхні різу. Це дозволяє знизити виробництво деталей та вузлів машин з конструкційних сталей великої товщини, для яких застосовується високопродуктивне термічне різання. Впровадження встановлених результатів досліджень у промислових умовах дозолить значно підвищити ефективність та продуктивність технологічного процесу за рахунок одержання високої якості поверхні

Ключові слова: термічне різання, зона термічного впливу, швидкість різання, кристалізація, металографічний аналіз

V. Kassov
Doctor of Technical Sciences, Professor*
E-mail: kassovvd@gmail.com
E. Gribkov
Doctor of Technical Sciences, Associate Professor, Head of Department
Department of Automated Metal Forming Process and Machinery**
E-mail: gribkov.eduard@gmail.com
O. Berezshnaya
Doctor of Technical Sciences*
E-mail: elena.kassova07@gmail.com
S. Malyhina
PhD, Associate Professor
Department of Computer and Information Technology**
E-mail: svmal5.sm@gmail.com
A. Sumets
PhD, Engineer
Mechanical Repair Shop
PSC «Severodonetsk Association «AZOT»
Pivovarova str., 5,
Severodonetsk, Ukraine, 93400
E-mail: avsumets@gmail.com
*Department of Handling Systems**
**Donbass State Engineering Academy
Akademichna str., 72,
Kramatrosk, Ukraine, 84313

1. Introduction

Plasma cutting has certain advantages over conventional methods of gas-flame and oxygen cutting. The prospects of this technology are predetermined by high energy parameters of the plasma cutting arc: volumetric concentration of power reaches 100–150 kW/cm^3, temperature is (5–16)·10^3 K, the rate of plasma flux outflow is up to 5,000 m/s, specific density of thermal power is (10–20) kW/mm^2. Due to such properties, plasma cutting is one of the most effective techniques for forming the shape of metals. High power concentration, the ability to control the process by changing the magnitude of a working current or the flow rate of plasma-forming gas, and, finally, the possibility of cutting almost any metals render universal technological capabilities to this technique.

Structural transformations under conditions of thermal cutting of a metal (argon-plasma, air-plasma, and oxygen-flux) are significantly different from transformations at standard heat treatment [1, 2]. These differences are explained, first of all, by the specificity of the thermal-deformational cutting cycle [3]. Under conditions of thermal cutting, decay of solid solutions in the cutting zone occurs

in a more complex environment that is constantly changing. In addition, the existence of chemical heterogeneity in the thermal heating zone radically alters the kinetics of decay of solid solutions in many cases [4, 5]. Therefore, the crystallization processes of a metal and the structural transformations in the cutting zone in most cases determine subsequent technological and operational properties of the metal. Thus, after cooling, the steel being cut is likely to have a heterogeneous or layered composition. Under such conditions for crystallization, if the doping element or admixture has greater solubility in the liquid phase than in the solid one, there occurs the enrichment of the inter-axial and inter-dendrite space. This would result in a substantial change in the structure with possible defect formation, which significantly affects subsequent performance of the metal. In addition, this would necessitate further technological operations for additional machining of the cut surface metal, which could increase the cost of manufacturing an article. Thus, it is a relevant task to comprehensively study the impact of the plasma cutting process on the structure formation of the melted metal.

2. Literature review and problem statement

As shown in paper [6], quality of the separating plasma cutting is characterized by the cut width, the magnitude of the non-perpendicular character of the lateral surfaces of the cut cavity, the roughness of the latter, the existence and size of a lattice, etc. From the point of view of thermophysics, the separating cutting of metals is the process of local heating, melting, and blowing of a metal from the frontal edge of the cut under exposure to the high temperature plasma jet [6]. In this case, the heat flow into a metal is predetermined by the radiant and convective heat exchange from the arc column, the arc spot, and a plasma jet behind the arc spot. According to [7], a radiant heat flow accounts for only five to ten percent of the total flow. Therefore, the size and shape of the heat flow into a metal is predetermined by the shape and character of arc behavior in the cutting cavity, which depend on the initial process parameters [7].

One of the important performance indicators for plasma cutting of metals is the retention of the starting properties of a metal near the cutting surface [7]. A powerful plasma arc, while melting a metal from the cut cavity, causes the emergence of a temperature field in the deeper and more distant layers of the metal. Moreover, this field is moved depending on the movement of a plasmatron, and its parameters depend on the power of the plasma arc, the thickness and type of the metal being cut, the speed of plasmatron displacement, as well as its structural and regime characteristics [7]. Under the influence of the emerging temperature field, there appears, in the metal, near the cutting surface, a thermal impact zone, which in terms of depth is divided into two characteristic sections [7].

As shown in study [8], the quality of surface roughness and the magnitude of a thermal impact zone at plasma cutting are affected by the speed and current of cutting, as well as the pressure of plasma and the distance from a cutter to the cutting surface. The cited study modeled the influence of process parameters on the quality indicators of cut surface. Paper [9] also reported mathematical treatment of experimental data using statistical methods. The disadvantages of these studies are the lack of examining the impact of process

parameters on structural transformations in the cutting zone. Research reported in [5–9] was also aimed at determining the influence of technological characteristics of the process on such quality indicators as the width of cutting and a thermal impact zone.

The impact of oxygen content in the plasma gas on the cuts in steel plates has been investigated in paper [10]. The authors reported experimental results on changes in the geometrical shape of cut edges when using nitrogen, air, and oxygen as plasma-forming gases. Study [11] compared three, most common in engineering, methods of thermal cutting – laser, plasma, and oxygen cutting, in terms of technical and economic indicators. However, such quality indicators as the roughness of the cutting surface, the width of a thermal impact zone, etc. were not considered. Authors of [12] reported the construction of a mathematical model for predicting a thermal impact zone at air-plasma cutting of an aluminum alloy. Optimal process parameters were determined; however, there are no such studies for ferrous metals. Work [13] experimentally investigated the influence of the process parameters of plasma cutting on the precision indicators of cut surface size. The authors examined the following process parameters: cutting speed, distance to a nozzle and arc voltage. The results from experimental studies into each of the three parameters of the process was statistically treated to derive general dependences.

The above indicators of thermal cutting quality are certainly important for determining the efficiency of a metal machining process. However, the process of metal crystallization after cutting is accompanied by many undesirable phenomena, including the formation of chemical heterogeneity [6, 7], which exerts significant effect on the performance characteristics of the material being cut. The formation of cutting edges is also characterized by the depth of a thermal impact zone and structure formation in this zone after thermal cutting. This necessitates subsequent machining of a material and affects the resulting cost of articles. The microscopic chemical heterogeneity, which emerges in a thermal cutting zone, is defined primarily by the character of primary crystallization of steel and depends on the amount and nature of alloying elements, impurities, and cooling conditions [5–8]. Therefore, it is important to study the influence of parameters for different methods of thermal cutting on regularities of structure formation for steels of varying degree of doping.

Thus, papers [14, 15] studied the influence of various types of cutting on the structure formation of bimetallic materials, as well as aluminum alloys. The authors examined the microstructures of cutting surfaces and measured microhardness for different cutting techniques. The impact of the type of cutting (mechanical or thermal) on the microstructure and change in the microhardness of cut surface of aluminum materials was determined. However, there are no such studies for ferrous metals of large thicknesses. In [16], authors reported results of high-precision plasma treatment of thin sheets made of bimetallic compositions obtained by a blast welding. The optimal technological and experimental process parameters were determined. The peculiarities of the formation of bimetallic sheets cut edges at plasma cutting were discussed in detail and the advantages of the process for materials of such class were given. However, up to now, the impact of cutting process parameters on the patterns in structure formation of a melted metal has remained insufficiently studied.

3. The aim and objectives of the study

The aim of this study is to identify patterns of structure formation in steels with a different degree of doping at different types of thermal cutting.

To accomplish the aim, the following tasks have been set:

– to study changes in the phase and structural transformations in the metal of samples made from constructional steels of different degree of doping at argon-plasma, air-plasma, and oxygen-flux cutting;

– to investigate the effect of the type of thermal cutting on the formation of a thermal impact zone and the distribution of microhardness on the cutting surface for steels with a varying degree of doping.

4. Methods and materials for experimental study into the influence of a metal treatment method on structure formation in a cutting area

The study was conducted under industrial conditions. Our experimental study into the influence of plasma cutting on structure formation in a cutting area involved the plasmatrons, which were mounted at the machine PPlKC-2,5 (Ukraine) (Fig. 1, Table 1). The PPlKC-2,5 machine of portal type consists of a portal, a rail track, a support, a CNC console, and an air-plasma cutting unit.

Fig. 1. Plasmatron mounted at the machine PPIKC-2,5

Our comparative assessment involved samples made from steel St 3sp, St 40, U10, 09G2S, 40Kh, 30Kh13, Kh12MF, 30KhMA, 25Kh1MF, 08Kh18N10T, 03Kh17N14M3, with the use of the following instruments: metallographic research was conducted using the optical mirror type microscope NEOFOT 21 (Ukraine); changes in microhardness were tested at PMT-3 (Ukraine); changes in the chemical composition were investigated using the spectroscope SPECTRO PORT (Belarus).

To run a metallographic analysis, we fabricated thin sections, 12×12 mm, by cutting a sample, grinding, and polishing its surface to a mirror luster. The cut samples were sharpened using an abrasive wheel (grain size 50 μm) with intermittent cooling, allowing overheating of the sample. The sharpened samples were sanded to complete removal of dashes. Next,

samples were exposed to etching in a 4 % solution of nitric acid in ethyl alcohol; that yielded the shape, size, and distribution of phases and structural components of the alloy. To determine microhardness, we fabricated thin sections in line with a similar procedure.

Table 1

Technical characteristics of the portal type CNC machine PPIKC-2,5

Largest size of machined sheets, mm:	
length	10,000
width	2,500
width:	
when cutting steel and aluminum from the sheet's edge	10–130
when cutting with copper punching	40
Accuracy of reproducing the assigned contour, mm	±0.35
Cutter displacement speed, mm/min	70–6,000
Number of supports	1
Machine dimensions, mm, not exceeding	4,700×11,600×1,860
Mass when delivered in assembly, kg	5,420

5. Results of experimental study into the influence of a metal treatment method on structure formation in the cutting zone

5. 1. Studying the changes in phase and structural transformations

At nonequilibrium crystallization, diffusion would not have time to align the composition of internal and external layers of a solid solution. Therefore, after cooling, the steel being cut would most likely demonstrate a heterogeneous or layered composition. Under such conditions for crystallization, if the alloying element or admixture has, in the liquid phase, a greater solubility than that in a solid one, there would occur the enrichment of the inter-axial and inter-dendrite space.

We studied peculiarities of structure formation in a thermal impact zone formed at thermal cutting by three types of cutting for 11 steel grades. Structural transformations under conditions of argon-plasma, air-plasma, and oxygen-flux cutting of metal are significantly different from transformations under conditional heat treatment. These differences are explained, first of all, by the specificity of the thermal-deformational cutting cycle [6].

Dendritic heterogeneity is well detected at the microstructure of a metal after thermal cutting, in the form of a surface relief (Fig. 3, *a, c*; Fig. 4, *c*; Fig. 5, *a*; Fig. 6, *a–c*; Fig. 7, *b–c*; Fig. 9, *a–b*; Fig. 11, *a–c*; Fig. 12, *a–c*).
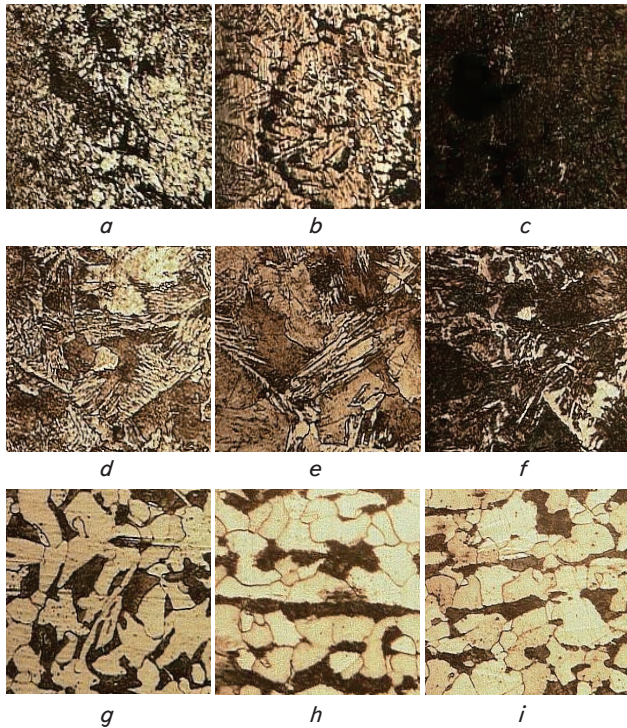
Fig. 2. Microstructure (×250) after different types of cutting: *a, d, g* — argon-plasma cutting; *b, e, h* — air-plasma cutting; *c, f, h* — oxygen-flux cutting; *a, b, c* — microstructure of melted section; *d, e, f* — microstructure of transitional section; *g, h, i* — microstructure of main metal
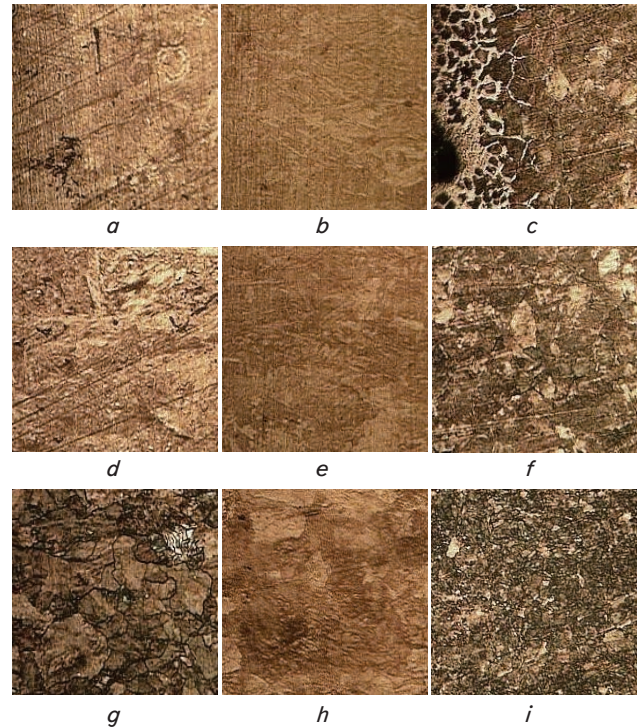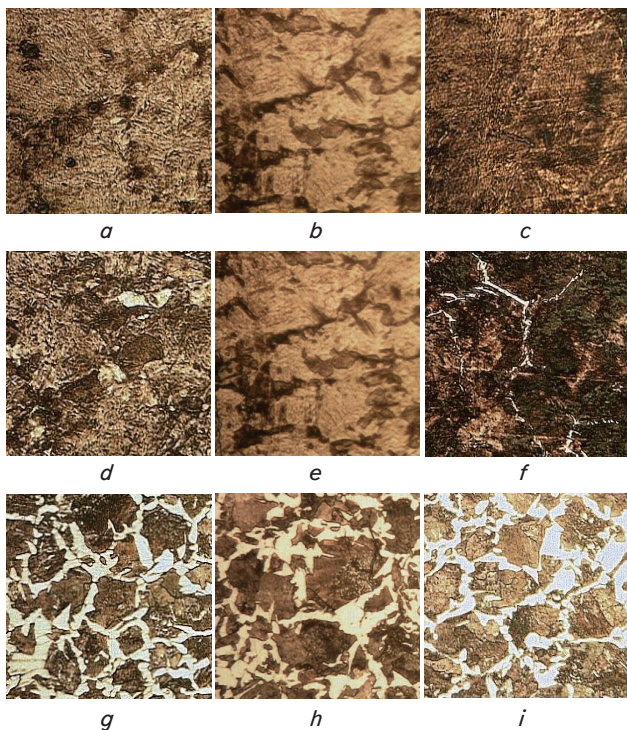

Fig. 4. Microstructure (×250) of steel U10 after different types of cutting: *a, d, g* — argon-plasma cutting; *b, e, h* — air-plasma cutting; *c, f, h* — oxygen-flux cutting; *a, b, c* — microstructure of melted section; *d, e, f* — microstructure of transitional section; *g, h, i* — microstructure of main metal

Fig. 3. Microstructure (×250) of steel 40 after different types of cutting: *a, d, g* — argon-plasma cutting; *b, e, h* — air-plasma cutting; *c, f, h* — oxygen-flux cutting; *a, b, c* — microstructure of melted section; *d, e, f* — microstructure of transitional section; *g, h, i* — microstructure of main metal
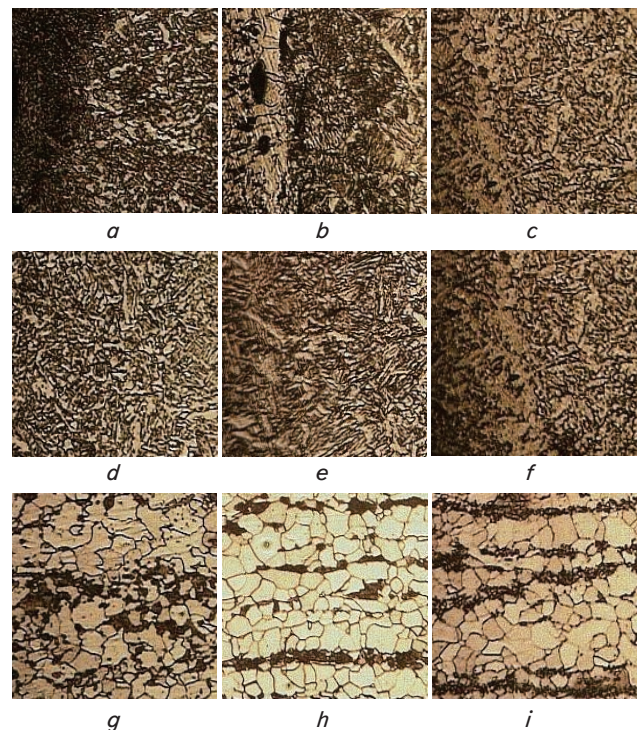

Fig. 5. Microstructure (×250) of steel 09G2S after different types of cutting: *a, d, g* — argon-plasma cutting; *b, e, h* — air-plasma cutting; *c, f, h* — oxygen-flux cutting; *a, b, c* — microstructure of melted section; *d, e, f* — microstructure of transitional section; *g, h, i* — microstructure of main metal

Fig. 6. Microstructure (×250) of steel 40Kh after different
types of cutting: *a, d, g* — argon-plasma cutting;
b, e, h — air-plasma cutting; *c, f, h* — oxygen-flux cutting;
a, b, c — microstructure of transitional section;
d, e, f — microstructure of transitional section;
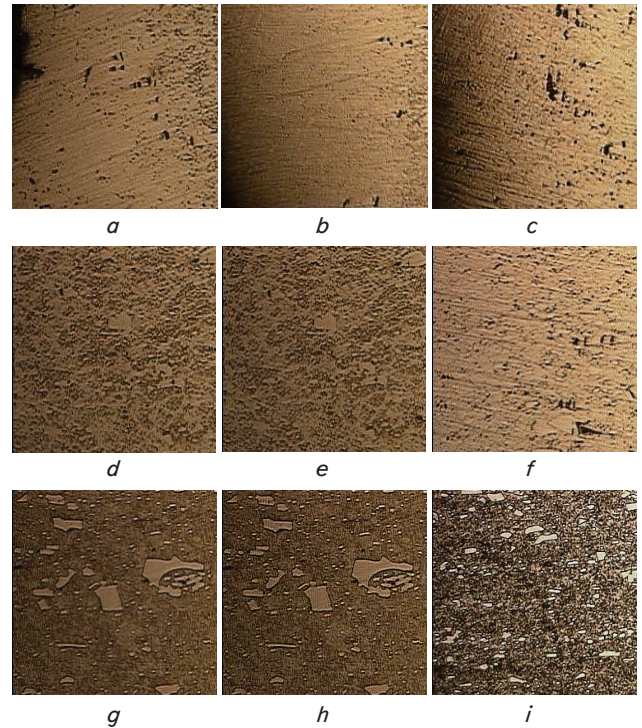*g, h, i* — microstructure of main metal

Fig. 8. Microstructure (×250) of steel Kh12MF after different
types of cutting: *a, d, g* — argon-plasma cutting;
b, e, h — air-plasma cutting; *c, f, h* — oxygen-flux cutting;
a, b, c — microstructure of melted section;
d, e, f — microstructure of transitional section;
g, h, i — microstructure of main metal

Fig. 7. Microstructure (×250) of steel 30Kh13 after different
types of cutting: *a, d, g* — argon-plasma cutting;
b, e, h — air-plasma cutting; *c, f, h* — oxygen-flux cutting;
a, b, c — microstructure of melted section;
d, e, f — microstructure of transitional section;
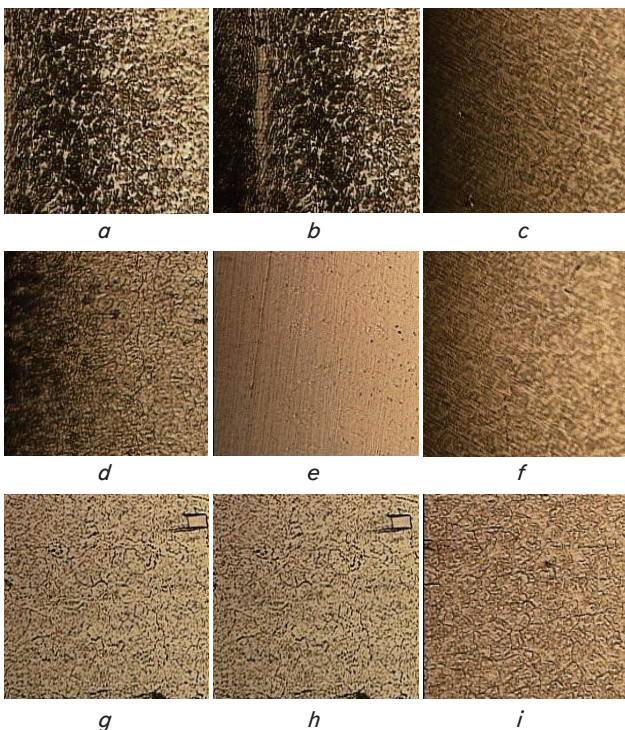*g, h, i* — microstructure of main metal

Fig. 9. Microstructure (×250) of steel 30KhMA after different
types of cutting: *a, d, g* — argon-plasma cutting;
b, e, h — air-plasma cutting; *c, f, h* — oxygen-flux cutting;
a, b, c — microstructure of melted section;
d, e, f — microstructure of transitional section;
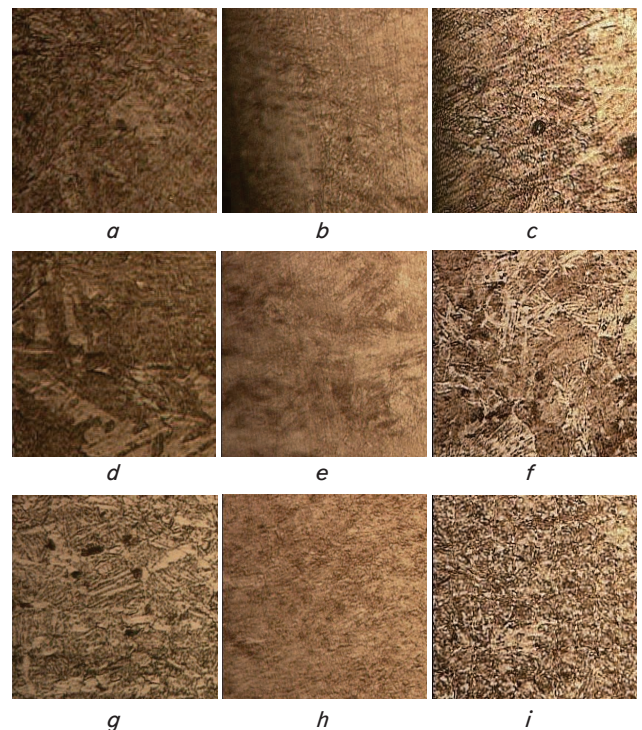*g, h, i* — microstructure of main metal

Fig. 10. Microstructure (×250) of steel 25Kh1MF
after different types of cutting: *a, d, g* — argon-plasma
cutting; *b, e, h* — air-plasma cutting; *c, f, h* — oxygen-flux
cutting; *a, b, c* — microstructure of melted section;
d, e, f — microstructure of transitional section;
g, h, i — microstructure of main metal
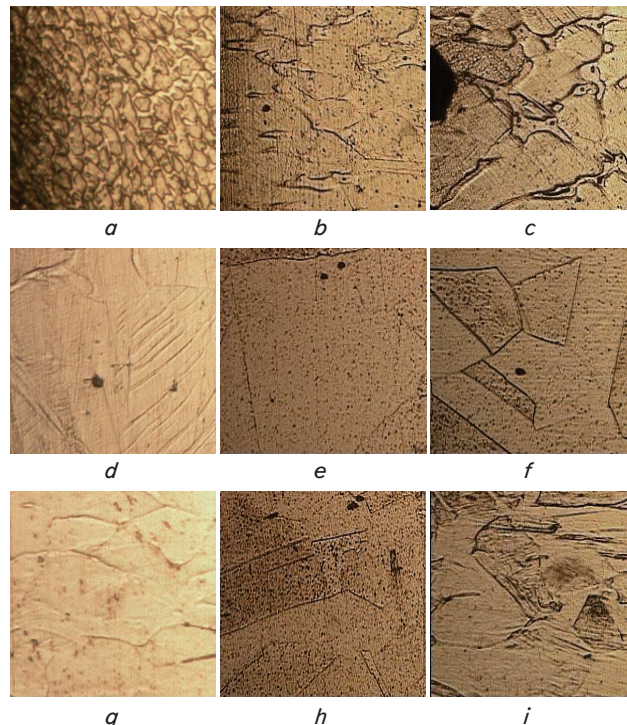
Fig. 12. Microstructure (×250) of steel 03Kh17N14M3
after different types of cutting: *a, d, g* — argon-plasma
cutting; *b, e, h* — air-plasma cutting; *c, f, h* — oxygen-flux
cutting; *a, b, c* — microstructure of melted section;
d, e, f — microstructure of transitional section;
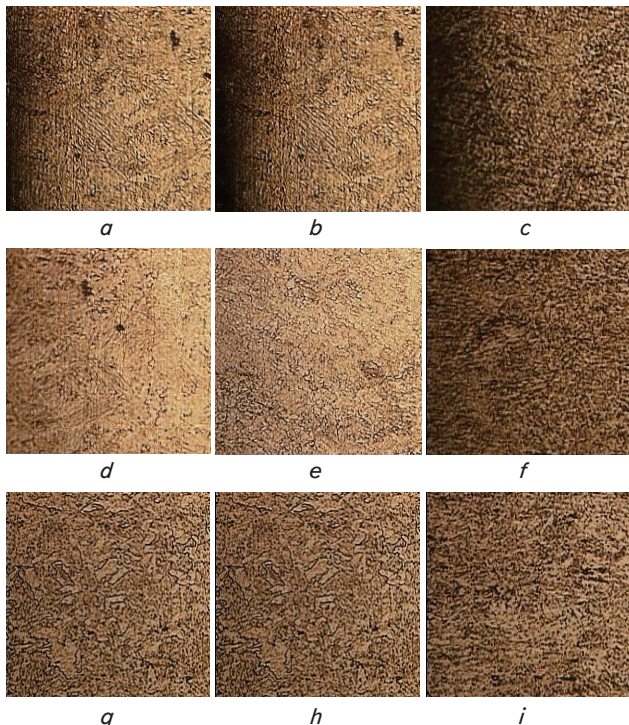*g, h, i* — microstructure of main meta

Fig. 11. Microstructure (×250) of steel 08Kh18N10T
after different types of cutting: *a, d, g* — argon-plasma
cutting; *b, e, h* — air-plasma cutting; *c, f, h* — oxygen-flux
cutting; *a, b, c* — microstructure of melted section;
d, e, f — microstructure of transitional section;
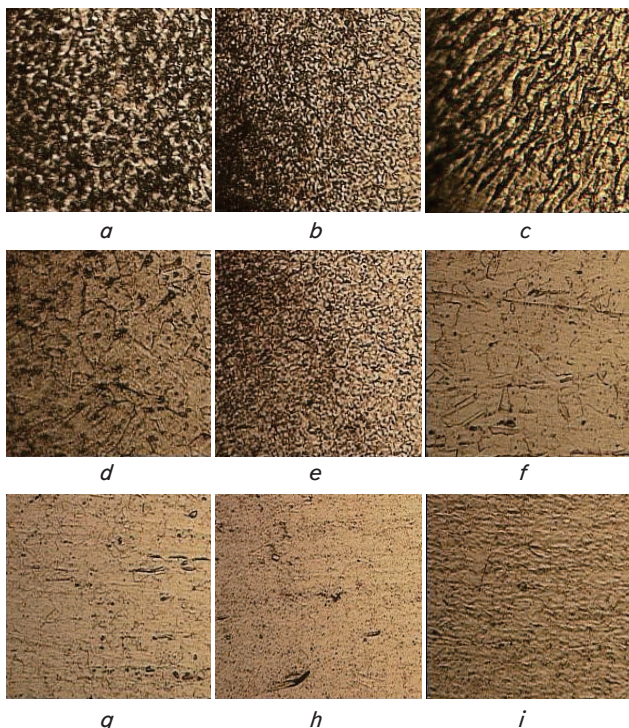*g, h, i* — microstructure of main metal

Under a very large enrichment, the inter-axial and inter-dendrite spaces demonstrate, during last stages of crystallization, irregular structures (Fig. 3, *a, c*; Fig. 4, *c*; Fig. 6, *a–c*; Fig. 9, *a*).

Tables 1, 2 give the impact of a cutting technique on the depth of thermally treated layers and microhardness.

The increase in the speed of cooling in the crystallization interval contributes to crushing of the primary metal structure in the cutting area, especially for alloyed steels (Fig. 3, *a, c*; Fig. 6, *b, e–f*).

5. 2. Studying the influence of the type of thermal cutting on the formation of a thermal impact zone and the distribution of microhardness on the cutting surface

The result of metallographic study is the established change in the depth of a thermal impact zone dependent on the type of thermal cutting for different grades of steel (Table 2).

The metal formed as a result of thermal cutting on the average-alloyed steels, cooled at elevated speeds, considerably exceeded the main metal in terms of microhardness indicators (Table 3).

Changes in microhardness occur not only as a result of crushing the primary structure, but also due to weakening the level of chemical heterogeneity, predetermined by the ratio of elements' concentrations in the liquation intra-crystalline layer and in the body of a columnar crystallite (Fig. 2, *a–c*; Fig. 4, *c*).

Table 4 gives microstructures formed at cutting different steels.

Table 2

Influence of cutting technique on the depth of thermally treated layers depending on steel grades

Cutting technique	Section	Depth of thermally treated layers, mm, for steel grades										
		3 sp.	40	U10	09G2S	40Kh	30Kh13	Kh12MF	30KhMA	25Kh1MF	08Kh18N10T	03Kh17N14M3
Argon plasma	MS	0.08	0.45	0.10	0.08	0.04	0.15	0.40	0.20	0.13	0.35	0.90
	TS	2.00	3.00	2.50	1.70	2.30	1.05	0.40	0.70	1.10	2.10	1.60
	Σ	2.08	3.45	2.60	1.78	2.34	1.20	0.80	0.90	1.23	2.45	2.50
Air plasma	MS	0.18	0.80	0.10	0.15	0.15	0.08	0.35	0.15	0.13	0.14	0.40
	TS	1.50	0.60	1.80	0.60	1.50	0.13	0.15	0.10	1.60	1.03	1.04
	Σ	1.68	1.40	1.90	0.75	1.65	0.21	0.50	0.25	1.73	1.17	1.44
Oxygen-flux	MS	0.10	0.25	0.05	0.50	0.40	0.13	0.58	0.15	0.18	0.43	2.72
	TS	1.50	7.00	1.40	2.00	1.70	2.15	1.70	3.20	1.70	4.30	3.30
	Σ	1.60	7.25	1.45	2.50	2.10	2.28	2.28	3.35	1.88	4.73	6.02

Note: MS – melted section, mm; TS – transitional section, mm; Σ – sum MS and TS

Table 3

Influence of cutting technique on microhardness depending on steel grades

Cutting technique	Section	microhardness, kg/mm^2 for steel grades										
		3sp.	40	U10	09G2S	40Kh	30Kh13	Kh12MF	30KhMA	25Kh1MF	08Kh18N10T	03Kh17N14M3
Argon plasma	MS	420	572	900	383	514	724	724	385	350	383	380
	TS	290	350	510	270	260	640	642	350	240	236	297
	MM	180	263	330	210	226	270	350	227	232	220	254
Air plasma	MS	170	572	420	193	420	824	950	383	350	272	254
	TS	220	322	380	200	380	640	642	383	237	274	254
	MM	180	263	330	210	226	270	350	227	232	220	254
Oxygen-flux	MS	193	322	824	181	464	642	724	383	420	383	274
	TS	210	275	500	160	350	724	946	350	382	279	274
	MM	180	263	330	210	226	270	350	227	232	220	254

Note: MS – melted section, mm; TS – transitional section, mm; MM – main metal

Table 4

Microstructures formed at cutting

Steel grade	Sections in a thermal impact zone												Main metal
	Melted section			Overheated section			Fine grain section			Section of incomplete recrystallization			
	Cutting type												
	A	B	K	A	B	K	A	B	K	A	B	K	A B K
3sp	M D W			M W			M W			M W			F P
40	D FS M	M S	D FS F M	FP W	S	S F M	F SS	S	SP FL	GP FL	S	GP S P FL	P FL
U10	M	T	M D C	T	T	M	T	T	M	T	T	M P	P
09G2S	FP D	FP B		FP W			FP SS			FP SS			FP SS
40Kh	F M D	M D FS	F M D	F M	M	F T	F S	F S FS	F S FS	F S SP			F SP
30Kh13	M A	HA D		M A	A		M A	A		M A	A		F KI
Kh12MF	HS			M KI			M KI			M KI			SP KI
30KhMA	M D	M D	M	M		T	M		F S	M		F S	F SP
25Kh1MF	M			F GP W	F S		F SP			F SP			F SP
08Kh18N10T	AF D	A D	AF D	A			A			A			A KI
03Kh17N14M3	HA D	HA D KI	HA D	A			A			A			A

Designations: *A* – argon plasma cutting, *B* – air-plasma cutting, *K* – oxygen-flux cutting, *FP* – ferrite-perlite structure, *D* – dendritic structure, *F* – ferrite, *SP* – sorbitol perlite, *GP* – granular perlite, *FL* – a ferrite lattice, *P* – perlite, *SC* – sorbitol. *W* – Widmanstätten pattern, *SS* – striped structure, *B* – burn, *AF* – austenitic-ferrite structure, *A* – austenitic structure, *HA* – heterogeneous austenitic solution, *C* – cementite, *HT* – high-temperature ferrite (δ). *DS* – dendritic structure of porous structure, *KI* – carbide and carbonitride inclusions, *M* – martensitic structure, *FS* – finely-dispersed structure, *T* – troostomartensite, *HS* – non-homogeneous solid solution (structure is poorly expressed)

6. Discussion of results of experimental study into the influence of a metal machining technique on structure formation in the cutting area

The result of thermal cutting is the established formation of conditional sections, starting from the melting zone to the main metal (Table 4).

The second section contains large grains. It includes a metal that was heated from a temperature of about 1,200 °C to the melting point of the main metal. Its width varies within 0.6−4.3 mm. When heated, metal undergoes α→λ transformations.

At overheating above the temperature of Ac3, the austenitic grain is growing and, even at a slight length of stay under high temperatures, manages to grow to impressive sizes (Fig. 11, 12, *d−f*). The type of the structure formed in the overheating area depends on the nature of the thermal process of cutting and the composition of a metal. Thus, in some cases, a Widmanstätten pattern (Fig. 3, *a*; Fig. 5, *d−f*) forms in this area.

In the alloyed steels, the metal sections heated at cutting above the temperature of AC3, acquire hardening structure as a result of rapid cooling (Fig. 6, *a−f*; Fig. 7, *a−e*; Fig. 9, *a−e*; Fig. 10, *a−c*).

However, the structure of the area for width from the site of fusion to the section, which was exposed at cutting to the maximum temperature slightly above Ac3AC3, would be the same. The result of the collapse of large austenitic grains in sections adjacent to the fusion border, which are heated at cutting above 12,00 °C, is the formation of larger coarse martensite (Fig. 10, *a−c*) than in the sections of metal heated at cutting above Ac3. The structure of the fusion zone is almost the same as the structure of the overheating area. The next section is the area of recrystallization. It includes a metal heated from a temperature slightly above the temperature of α→transformation, to 1,100−1,150 °C. The width of a given section is 0.7−1.0 mm.

In the low carbon and low-alloyed steels, in the section of recrystallization, there is usually a fine-dispersed (granular) structure formed (Fig. 3, *a*, *c*), which characterizes in general a sufficiently high range of mechanical properties. In the medium and high-alloyed steels, in the metal of a given area, there often forms a fine-plate martensite or a mixture of martensite and products of intermediate conversion (Fig. 7, *d*; Fig. 8, 9, *d−f*), that is the same structures as in the area of overheating, but more dispersed.

The next, fourth section, contains a metal heated from Ac1 temperature to a temperature of Ac3AC3. The metal within this section undergoes only partial recrystallization; therefore, it can be termed a section of incomplete recrystallization. The metal of this section in low carbon and low-alloyed steels is characterized by almost unchanged ferrite grain (Fig. 6, *d−f*) and some crushing, as well as the spheroidization of perlite sections (Fig. 4, *f*; Fig. 6, *d−f*). In the medium- and high-alloyed steels, after cooling, there forms the structure of partial hardening (Fig. 7, *d*; Fig. 8, *d−f*; Fig. 9, *d−e*).

The next section, fourth, can be termed a recrystallization section. It includes the metal that was heated from 500 °C to temperatures slightly below Ac1. Separate sections of a given zone, heated below Ac1, in terms of their structure and properties, may be different depending on the starting state of a metal before thermal cutting. If a metal underwent, before cutting, cold plastic deformation, then, when heated to temperatures below Ac1AC1, there is recrystallization, which leads to significant grain growth (Fig. 11, 12, *d−f*). The sixth section includes the metal, which was heated in the temperature range of 100−500 °C. This section in the process of cutting does not undergo visible structural changes (Fig. 5, 10, *d−f*). High-alloyed austenitic steels do not undergo visible phase transformations when exposed to thermal influence at cutting. Consequently, a zone of thermal heating of these steels has a less complex structure (Fig. 11, 12) than the zone at cutting conditional constructional steels (Fig. 3, 5, 7). The size of the high-alloyed steel fusion zone is relatively small and is determined by a temperature gradient and the crystallization interval. If the temperature gradient is small and the crystallization interval is relatively large, the width of the fusion zone grows. The properties of a thermal impact zone at cutting are inextricably linked with the condition of grain boundaries in it. In the zone of thermal influence, under the influence of thermal cycle of cutting, there is an energetic grain growth (Fig. 10, 11, *d−f*), as well as the smelting of boundaries in a fusion zone (Fig. 2, 4, *c*) and the subsequent development of chemical microheterogeneity in it (Fig. 4, *c*). In this regard, along the grain boundaries, there are the localized various kinds of destruction, which exerts a significant impact on their mechanical properties. In the fusion zone, the boundaries of two types are formed – primary and secondary. The primary boundaries form smaller grains (Fig. 6, *e*, *f*), secondary – (thin) large grains (Fig. 10, *e*, *f*). Primary and secondary boundaries are typically located arbitrarily in relation to each other. Primary boundaries contain an increased number of alloying elements, and the level of chemical heterogeneity can be compared with dendritic heterogeneity, which is developed in the crystallization of the fusion zone. This suggests that primary boundaries occur as a result of formation and subsequent solidification of the liquid phase. The latter is convincingly confirmed by data from metallographic study (Fig. 2−12; Table 4) and measurements of microhardness (Table 3). Thus, it has been determined that the depth of a thermal impact zone obtained at air-plasma cutting is much smaller in comparison with other types of cutting.

The method of microstructural analysis helped us establish that the most effective and appropriate type of steel cutting is air-plasma cutting by plasmatrons (Fig. 2−12, *b*, *e*, *h*). According to the derived data, the depth of thermal impact zone for different types of thermal cutting varies for different grades of steel similarly to the value of microhardness in obtained samples. However, a general regularity appears, indicating that at air-plasma cutting one observes a less depth of thermally treated metal layers. Microhardness for both high alloy and carbon steels at air-plasma cutting is significantly lower than, for example, at argon-plasma cutting. The structures formed in a thermal impact zone, as well as the character and depth of a given zone, testify to the selection of air plasma cutting (Tables 2−4). Such indicators of microhardness and the depth of a thermal impact zone in samples, which were exposed to air-plasma cutting, could simplify subsequent mechanical treatment of cut surface, which would affect the cost of resulting articles.

7. Conclusions

1. Our study has shown that high-alloyed austenitic steels do not undergo visible phase transformations when

exposed to thermal influence at cutting. Consequently, the zone of thermal heating of these steels has a less complicated structure than the zone at cutting conditional constructional steels.

2. It has been determined that the most efficient and appropriate type of steel cutting is air-plasma cutting by plasmatrons. We have performed metallographic research and obtained results from measuring microhardness, studied the structure and depth of thermally treated layers in a thermal impact zone for 11 steel grades by using argon-plasma, air-plasma, oxygen-flux cutting. It is shown that microhardness in the zone of a melted section at air-plasma cutting is 1.2–1.5 times less than that at argon-plasma cutting, and is 1.8–2.1 times less than that at oxygen-flux cutting. It has been established that the depth of a thermal impact zone at air-plasma cutting is less than other types of machining at cutting metals of large thickness (by 2–4 times less compared to argon-plasma and oxygen-flux cutting). Application of air-plasma cutting as a technological operation could significantly reduce the cost of subsequent machining of billets and rationally plan the technological process at the stage of its development.

References

1. Anakhov, S. V., Pyckin, Y. A., Matushkin, A. V. (2016). Narrow Jet Plasma as the Energy Efficient and Safe Technology for Metal Cutting. Materials Science Forum, 870, 523–527. doi: https://doi.org/10.4028/www.scientific.net/msf.870.523

2. Novosel'tsev, Y. G., Vasil'ev-Polikin, K. S., Krylov, V. M., Tuf, S. M. (2013). Analysis of the conditions of efficient and stable operation of plasma in welding processes. Welding International, 27 (2), 136–138. doi: https://doi.org/10.1080/09507116.2012.695544

3. Salonitis, K., Vatousianos, S. (2012). Experimental Investigation of the Plasma Arc Cutting Process. Procedia CIRP, 3, 287–292. doi: https://doi.org/10.1016/j.procir.2012.07.050

4. Das, M. K., Kumar, K., Barman, T. K., Sahoo, P. (2014). Optimization of Process Parameters in Plasma arc Cutting of EN 31 Steel Based on MRR and Multiple Roughness Characteristics Using Grey Relational Analysis. Procedia Materials Science, 5, 1550–1559. doi: https://doi.org/10.1016/j.mspro.2014.07.342

5. Ramakrishnan, H., Balasundaram, R., Ganesh, N., Karthikeyan, N. (2018). Experimental investigation of cut quality characteristics on SS321 using plasma arc cutting. Journal of the Brazilian Society of Mechanical Sciences and Engineering, 40 (2). doi: https://doi.org/10.1007/s40430-018-0997-8

6. Loktionov, A., Gaar, N. (2015). Influence of Technological Parameters of High-Precision Plasma Cutting on the Position of the Anode Spot on the Cut Edge. Applied Mechanics and Materials, 788, 46–51. doi: https://doi.org/10.4028/www.scientific.net/amm.788.46

7. Yuan, X. Q., Li, H., Zhao, T. Z., Wang, F., Guo, W. K., Xu, P. (2004). Comparative Study of Flow Characteristics Inside Plasma Torch with Different Nozzle Configurations. Plasma Chemistry and Plasma Processing, 24 (4), 585–601. doi: https://doi.org/10.1007/s11090-004-7934-6

8. Schitsin, Y. D., Kuchaev, P. S., Schitsin, V. Y. (2013). Plasma cutting of metals with reversed polarity and mixed supply of gases. Welding International, 27 (11), 890–892. doi: https://doi.org/10.1080/09507116.2013.796640

9. Krivonosova, E. A., Schitsin, Y. D., Trushnikov, D. N., Myshkina, A. V., Akulova, S. N., Neulibin, S. D., Dushina, A. Y. (2018). Structure formation of high-temperature alloy by plasma, laser and TIG surfacing. Journal of Physics: Conference Series, 1089, 012019. doi: https://doi.org/10.1088/1742-6596/1089/1/012019

10. Ramakrishnan, S., Shrinet, V., Polivka, F. B., Kearney, T. N., Koltun, P. (2000). Influence of gas composition on plasma arc cutting of mild steel. Journal of Physics D: Applied Physics, 33 (18), 2288–2299. doi: https://doi.org/10.1088/0022-3727/33/18/313

11. Harničárová, M., Valíček, J., Zajac, J., Hloch, S., Čep, R., Džubáková, I. et. al. (2012). Techno-economical comparison of cutting material by laser, plasma and oxygen. Tehnički vjesnik, 19, 813–817.

12. Kadirgama, K., Noor, M. M., Harun, W. S. W., Aboue-El-Hossein, K. A. (2010). Optimisation of heat affected zone by partial swarm optimisation in air plasma cutting operation. Journal of Scientific and Industrial Research, 69, 439–443.

13. Kechagias, J., Petousis, M., Vidakis, N., Mastorakis, N. (2017). Plasma Arc Cutting Dimensional Accuracy Optimization employing the Parameter Design approach. ITM Web of Conferences, 9, 03004. doi: https://doi.org/10.1051/itmconf/20170903004

14. Rakhimyanov, K., Rakhimyanov, A., Heifetz, M. (2015). High-Precision Plasma Cutting of the Steel – Aluminum «Bimetallic Composition». Applied Mechanics and Materials, 788, 41–45. doi: https://doi.org/10.4028/www.scientific.net/amm.788.41

15. Akkurt, A. (2015). The effect of cutting process on surface microstructure and hardness of pure and Al 6061 aluminium alloy. Engineering Science and Technology, an International Journal, 18 (3), 303–308. doi: https://doi.org/10.1016/j.jestch.2014.07.004

16. Rakhmyanov, K., Rakhmyanov, A., Zhuravlev, A. (2014). Advantages of High-Precision Plasma Cutting for Processing Bimetallic Compositions. Applied Mechanics and Materials, 698, 294–298. doi: https://doi.org/10.4028/www.scientific.net/amm.698.294